

Selective Kernel Attention for Robust Speaker Verification

Sung Hwan Mun^{1,*}, Jee-weon Jung^{2,*} and Nam Soo Kim¹

¹Dept. of ECE and INMC, Seoul National University, Seoul 08826, South Korea

²Naver Corporation, South Korea

shmun@hi.snu.ac.kr, jeeveon.jung@navercorp.com, nkim@snu.ac.kr

Abstract

Recent state-of-the-art speaker verification architectures adopt multi-scale processing and frequency-channel attention techniques. However, their full potential may not have been exploited because these techniques' receptive fields are fixed where most convolutional layers operate with specified kernel sizes such as 1, 3 or 5. We aim to further improve this line of research by introducing a selective kernel attention (SKA) mechanism. The SKA mechanism allows each convolutional layer to adaptively select the kernel size in a data-driven fashion based on an attention mechanism that exploits both frequency and channel domain using the previous layer's output. We propose three module variants using the SKA mechanism whereby two modules are applied in front of an ECAPA-TDNN model, and the other is combined with the Res2Net backbone block. Experimental results demonstrate that our proposed model consistently outperforms the conventional counterpart on the three different evaluation protocols in terms of both equal error rate and minimum detection cost function. In addition, we present a detailed analysis that helps understand how the SKA module works.

Index Terms: speaker verification, selective kernel attention, multi-scale module

1. Introduction

In recent years, various deep neural network architectures for speaker verification (SV) systems have been proposed [1–6]. Current state-of-the-art architectures typically utilise 1-dimensional convolutional neural networks (1D-CNN) such as x-vector, RawNet3, or ECAPA-TDNN [7–9]. Among these, ECAPA-TDNN [9] is widely adopted, demonstrating stable yet competitive performance across a wide range of studies. It involves Res2Net backbone blocks with a squeeze-excitation (SE) layer at the end of each block, where the Res2Net incorporates multi-scale modelling and the SE efficiently recalibrates the channel (filter) axis of a CNN feature map [10, 11].

Several architectures that extend ECAPA-TDNN are also being proposed [12, 13]. In [12], ECAPA-CNN-TDNN extended ECAPA-TDNN by adding a 2D CNN-based front-end with frequency-wise SE layers to incorporate frequency translational invariance. Similarly, MFA-TDNN [13] applied a 2D-CNN-based module in front of the original ECAPA-TDNN identical to the ECAPA-CNN-TDNN; however, it proposed to replace the 2D-CNN-based module with a multi-scale frequency-channel attention module. Leveraging the multi-scale processing capability and the attention module, which resembles the SE layer, MFA-TDNN demonstrates competitive performance across test scenarios involving diverse duration.

To this end, we propose to further push this line of research by introducing a selective kernel attention (SKA) mechanism

*Equal contribution

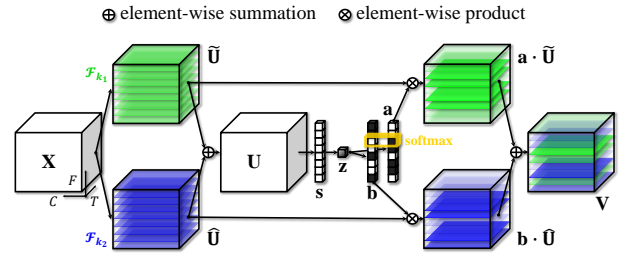


Figure 1: Selective kernel attention (SKA) module.

inspired by [14, 15]. Speech signals have multi-scale and hierarchical linguistic structures (e.g., phoneme, syllable, and word) and different time-frequency responses. Thus, the local and global information should be adaptively emphasised to extract robust speaker-discriminative representations [16]. Introducing the SKA mechanism, our proposed module can include several different-sized kernels and also choose which kernel to concentrate on in a *data-driven* fashion.

Hence, we argue that our proposed SKA module can efficiently address the local and global input data information and further strengthen multi-scale processing capability compared to the previous works, which only depend on a naive 2D-CNN or Res2Net architecture. In addition, we incorporate the SKA approach with the Res2Net-based backbone blocks, expecting that it would also result in a neural architecture that can better model utterances with diverse durations. Vast experiments conducted using three different evaluation protocols consistently demonstrate that our proposed SKA module outperforms the baseline systems. In addition, we observe the identical tendency across three different durations.

The rest of this paper is organised as follows: Section 2 describes the selective kernel attention module, and Section 3 presents the proposed architectures. Then, the experiments and results are addressed in Sections 4 and 5, respectively. Finally, we conclude in Section 6.

2. Selective kernel attention module

This Section describes the selective kernel attention (SKA) mechanism, illustrated in Figure 1, that can select the kernel size adaptive in a data-driven fashion. The three sub-sections address different SKA variants where the first two variants exist before backbone blocks, and the last variant is utilised within each backbone block.

2.1. 2D CNN-based channel-wise SKA (cwSKA)

For a given $\mathbf{X} \in \mathbb{R}^{C' \times F' \times T'}$, let $\mathcal{F}_{k_1} : \mathbf{X} \rightarrow \tilde{\mathbf{U}} \in \mathbb{R}^{C \times F \times T}$ and $\mathcal{F}_{k_2} : \mathbf{X} \rightarrow \hat{\mathbf{U}} \in \mathbb{R}^{C \times F \times T}$ be two convolution opera-

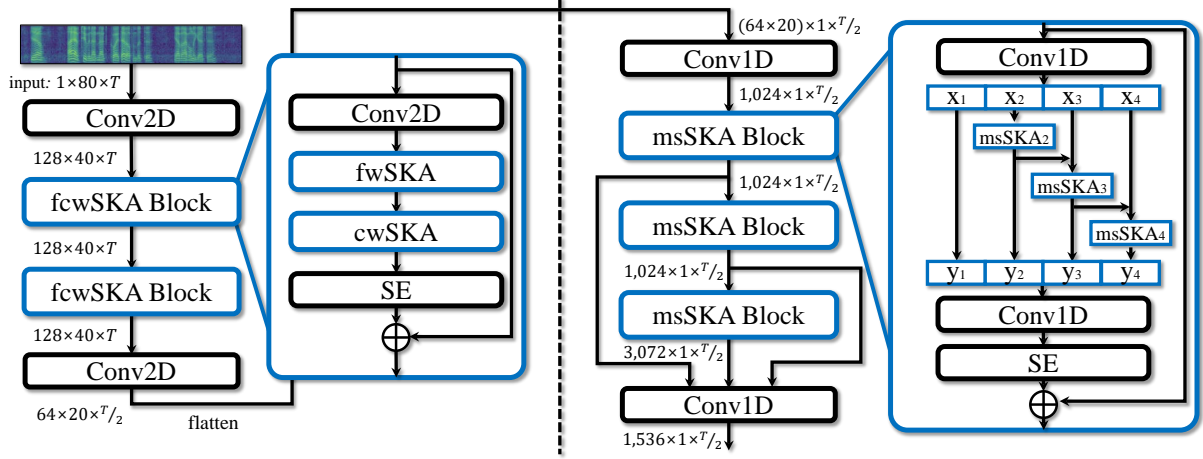


Figure 2: The overall proposed architecture: The frequency-channel-wise SKA block-based front network (left) and the multi-scale SKA block-based TDNN network (right). The total architecture is referred to SKA-TDNN msSKA.

tors with kernel sizes k_1 and k_2 , respectively. First, the input feature map \mathbf{X} is split into two branches $\tilde{\mathbf{U}}$ and $\hat{\mathbf{U}}$ by two operators \mathcal{F}_{k_1} and \mathcal{F}_{k_2} , respectively. To integrate different scales of information into the next layer, two branches are fused by an element-wise summation, i.e., $\mathbf{U} = \tilde{\mathbf{U}} + \hat{\mathbf{U}}$. Then 2D global average pooling (GAP) embeds the global information into the channel-wise feature vector \mathbf{s} as follow:

$$\mathbf{s}_c = \mathcal{F}_{gp}(\mathbf{U}_c) = \frac{1}{F \times T} \sum_{i=1}^F \sum_{j=1}^T \mathbf{U}_c(i, j). \quad (1)$$

The fully-connected (FC), batch normalisation (BN) and ReLU layers are sequentially passed to squeeze the channel-wise compact feature \mathbf{z} , i.e., $\mathbf{z} = \text{ReLU}(\text{BN}(\mathbf{W}\mathbf{s}))$, where $\mathbf{W} \in \mathbb{R}^{d_c \times C}$ denotes the weight matrix of a FC layer. Next, soft attention weights across channels are calculated via a softmax function as follows:

$$\mathbf{a}_c = \frac{e^{\mathbf{A}_c \mathbf{z}}}{e^{\mathbf{A}_c \mathbf{z}} + e^{\mathbf{B}_c \mathbf{z}}}, \quad \mathbf{b}_c = \frac{e^{\mathbf{B}_c \mathbf{z}}}{e^{\mathbf{A}_c \mathbf{z}} + e^{\mathbf{B}_c \mathbf{z}}}, \quad (2)$$

where $\mathbf{A}, \mathbf{B} \in \mathbb{R}^{C \times d_c}$ are the FC weights and $\mathbf{a}, \mathbf{b} \in \mathbb{R}^{C \times 1}$ denote the channel-wise soft attention vector for $\tilde{\mathbf{U}}$ and $\hat{\mathbf{U}}$, respectively. $\mathbf{a}_c, \mathbf{b}_c$ are the c -th elements of \mathbf{a}, \mathbf{b} and $\mathbf{A}_c, \mathbf{B}_c \in \mathbb{R}^{1 \times d_c}$ denote the c -th row vectors of \mathbf{A}, \mathbf{B} , respectively.

Finally, the output feature map $\mathbf{V} \in \mathbb{R}^{C \times F \times T}$ is computed as the weighed summation over the different branches as:

$$\mathbf{V}_c = \mathbf{a}_c \cdot \tilde{\mathbf{U}}_c + \mathbf{b}_c \cdot \hat{\mathbf{U}}_c, \quad \mathbf{a}_c + \mathbf{b}_c = 1, \quad (3)$$

where $\mathbf{V}_c \in \mathbb{R}^{F \times T}$ is the c -th component of \mathbf{V} . Note that SKA can also be extended to a multi-branch variant that involves three or more branches.

2.2. 2D CNN-based frequency-wise SKA (fwSKA)

Channel-wise SKA extracts the global information regarding the channel importance by using 2D GAP on the $F \times T$ dimension. However, we argue that speaker-discriminative information also exists in the frequency or temporal domain, which the channel-wise recalibration can not effectively capture. Thus,

we propose to aggregate global frequency information to the attention weights using the SKA framework:

$$\mathbf{s}_f = \mathcal{F}_{gp}(\mathbf{U}_f) = \frac{1}{C \times T} \sum_{i=1}^C \sum_{j=1}^T \mathbf{U}_f(i, j), \quad (4)$$

where \mathbf{s}_f denotes the f -th element of frequency-wise feature vector $\mathbf{s} \in \mathbb{R}^{F \times 1}$. The values of the frequency-wise compact feature $\mathbf{z} \in \mathbb{R}^{d_f \times 1}$, soft attention vectors $\mathbf{a}, \mathbf{b} \in \mathbb{R}^{F \times 1}$, and output feature map $\mathbf{V} \in \mathbb{R}^{C \times F \times T}$ are obtained in the same way as in equation (1), (2), and (3), respectively.

We first emphasise the frequency axis of a 3D CNN feature map via fwSKA and sequentially recalibrate the channel axis via cwSKA. This frequency-channel-wise SKA module is referred to as fcwSKA.

2.3. 1D CNN-based multi-scale SKA (msSKA)

The two variants of the SKA mechanism target 2D-CNNs, whereas we believe that the SKA mechanism can also be helpful for a module that composes residual backbone blocks, enhancing the module to process multi-scale data more efficiently. Thus, we introduce a 1D CNN-based multi-scale SKA module. First, in the front of multi-scale module, a 2D input feature map $\mathbf{X} \in \mathbb{R}^{C \times T}$ is evenly divided into s feature map subsets $\mathbf{x}_i \in \mathbb{R}^{C/s \times T}$ where s denotes the number of scales and $i \in \{1, 2, \dots, s\}$. Using a 1D GAP, the i -th scale's feature vector \mathbf{s}^i is obtained as:

$$\mathbf{s}_c^i = \mathcal{F}_{gp}(\mathbf{U}_c^i) = \frac{1}{T} \sum_{k=1}^T \mathbf{U}_c^i(k), \quad (5)$$

where $\mathbf{U}^i \in \mathbb{R}^{C/s \times T}$ is the i -th scale's fused feature map obtained via 1D-CNN with different kernel sizes. Also, the i -th scale's values of the compact feature $\mathbf{z}^i \in \mathbb{R}^{d_c/s \times 1}$, the soft attentions $\mathbf{a}^i, \mathbf{b}^i \in \mathbb{R}^{C/s \times 1}$, and the output feature map $\mathbf{V}^i \in \mathbb{R}^{C/s \times F \times T}$ are calculated as in the Section 2.1 and 2.2.

3. Model architectures

Figure 2 illustrates the overall scheme of the proposed architecture. We propose two modules leveraging the SKA mechanism

Table 1: The experimental results on the VoxCeleb1-O, VoxCeleb-E and VoxCeleb-H evaluation protocols. TTA: Test time augmentation. SN: Adaptive score normalisation. †: Our implementation.

Model		VoxCeleb1-O						VoxCeleb1-E						VoxCeleb1-H					
		EER(%)			MinDCF			EER(%)			MinDCF			EER(%)			MinDCF		
		Full	3.0s	1.5s	Full	3.0s	1.5s	Full	3.0s	1.5s	Full	3.0s	1.5s	Full	3.0s	1.5s	Full	3.0s	1.5s
ResNet34 H/ASP [6]	-	1.09	1.47	2.67	0.091	0.112	0.200	1.28	1.59	2.64	0.094	0.114	0.184	2.29	2.95	4.68	0.167	0.200	0.293
	+TTA	1.06	-	-	0.083	-	-	1.23	-	-	0.087	-	-	2.23	-	-	0.155	-	-
	+SN	1.01	1.31	2.55	0.080	0.108	0.193	1.14	1.46	2.51	0.080	0.103	0.171	2.55	2.96	4.78	0.133	0.178	0.272
ECAPA-TDNN† [9]	-	1.01	1.43	2.77	0.081	0.110	0.197	1.21	1.52	2.75	0.088	0.105	0.183	2.23	2.89	4.72	0.156	0.201	0.296
	+TTA	0.97	-	-	0.078	-	-	1.19	-	-	0.086	-	-	2.14	-	-	0.150	-	-
	+SN	0.96	1.35	2.59	0.077	0.105	0.188	1.16	1.48	2.60	0.079	0.101	0.179	2.10	2.79	4.59	0.135	0.181	0.274
ECAPA-CNN-TDNN† [12]	-	0.94	1.21	2.32	0.063	0.095	0.172	1.07	1.39	2.36	0.074	0.096	0.159	2.03	2.64	4.34	0.129	0.169	0.255
	+TTA	0.91	-	-	0.063	-	-	1.06	-	-	0.071	-	-	2.04	-	-	0.123	-	-
	+SN	0.88	1.20	2.26	0.060	0.094	0.168	1.01	1.35	2.31	0.069	0.092	0.154	1.93	2.52	4.11	0.115	0.160	0.247
MFA-TDNN† [13]	-	0.90	1.18	2.28	0.064	0.096	0.169	1.05	1.36	2.33	0.073	0.097	0.161	2.00	2.62	4.29	0.132	0.165	0.252
	+TTA	0.86	-	-	0.068	-	-	1.03	-	-	0.070	-	-	2.02	-	-	0.130	-	-
	+SN	0.84	1.16	2.20	0.059	0.092	0.161	0.98	1.30	2.27	0.066	0.093	0.152	1.89	2.48	3.98	0.119	0.158	0.243
ECAPA-TDNN msSKA	-	0.97	1.29	2.45	0.074	0.107	0.181	1.13	1.47	2.52	0.076	0.099	0.168	2.12	2.76	4.49	0.153	0.186	0.268
	+TTA	0.95	-	-	0.076	-	-	1.12	-	-	0.078	-	-	2.10	-	-	0.148	-	-
	+SN	0.92	1.28	2.41	0.072	0.099	0.175	1.09	1.44	2.48	0.074	0.096	0.164	2.01	2.65	4.38	0.130	0.175	0.265
SKA-TDNN	-	0.87	1.18	2.20	0.059	0.084	0.160	0.99	1.29	2.19	0.069	0.091	0.148	1.90	2.44	4.00	0.118	0.154	0.246
	+TTA	0.84	-	-	0.055	-	-	0.98	-	-	0.067	-	-	1.89	-	-	0.114	-	-
	+SN	0.80	1.14	2.07	0.057	0.080	0.152	0.93	1.20	2.06	0.061	0.084	0.137	1.77	2.31	3.79	0.104	0.143	0.232
SKA-TDNN msSKA	-	0.85	1.14	2.14	0.054	0.082	0.154	0.97	1.25	2.12	0.065	0.087	0.144	1.87	2.41	3.95	0.114	0.150	0.241
	+TTA	0.83	-	-	0.053	-	-	0.94	-	-	0.063	-	-	1.85	-	-	0.111	-	-
	+SN	0.78	1.10	2.05	0.047	0.078	0.147	0.90	1.18	2.03	0.059	0.081	0.134	1.74	2.28	3.77	0.102	0.138	0.224

described in the previous Section: fcwSKA block and msSKA block.

The fcwSKA block. comprises two 2D-CNNs and two proposed fcwSKA blocks. Each fcwSKA block includes a 2D-CNN, fwSKA, cwSKA, SE layers sequentially with the residual connection.

The msSKA block. resembles a typical Res2Net backbone block. However, we adopt msSKA to each *scale* except one.

By applying either module or both to the ECAPA-TDNN architecture, we propose three systems:

- **ECAPA-TDNN msSKA.** does not employ a 2D CNN-based module in front of the ECAPA-TDNN. It replaces the backbone blocks with the msSKA-based block (Figure 2, right). In each msSKA module, we use the 1D-CNNs with kernel sizes of 3 and 5 for the selective convolution. Both the dilation and group size are set to 1, and the reduction ratio C/d_c is 8. We adopt a channel of 1,024 and a scale of 8.
- **SKA-TDNN.** places the proposed fcwSKA block-based front module before the standard ECAPA-TDNN (Figure 2 left). In each fcwSKA module, the 2D-CNNs with the kernel sizes of 3×3 and 5×5 are exploited. In addition, the dilation, the group size, and the reduction ratio are set to the same values as in the ECAPA-TDNN msSKA. For the ECAPA-TDNN, a channel of 1,024 and a scale of 8 are used.
- **SKA-TDNN msSKA.** consists of both the fcwSKA block-based front and the msSKA block-based TDNN network (Figure 2). We set the hyper-parameters to the same values used in the ECAPA-TDNN msSKA and the SKA-TDNN.

We adopt the channel and context-dependent statistic pooling [9] to aggregate the frame-level output features in all systems. We adopt the equal-weighted summation of the additive angular margin (AAM) softmax [17] and the angular prototypical (AP) [5] objective functions to train all networks.

4. Experiments

4.1. Baseline model architectures

We utilise four baselines: ResNet34 H/ASP [6], ECAPA-TDNN [9], ECAPA-CNN-TDNN [12] and MFA-TDNN [13]. We use the pre-trained weight parameters for ResNet34 H/ASP and re-implement the remaining three baselines.

4.2. Dataset and evaluation protocol

We use the development set of VoxCeleb2 dataset [4] for training the models, which consists of 1,092,009 utterances from 5,994 speakers. The evaluation is performed using VoxCeleb1 dataset [3] where we report the equal error rate (EER) and the minimum detection cost function (MinDCF) for three different evaluation protocols, namely, VoxCeleb1-O, VoxCeleb1-E and VoxCeleb1-H. $P_{target}=0.05$ and $C_{miss}=C_{fa}=1$ are used to calculate the MinDCF metric.

4.3. Back-end approaches for the scoring

We report the performance of each model using three different back-end methods: vanilla cosine similarity, test time augmentation (TTA), and score normalisation (SN). We input the whole utterance at once for the vanilla cosine similarity and extract an embedding. For the TTA [4], we first segment each utterance into ten 4 seconds segments with the overlaps. The score for a given trial is derived by averaging cosine similarity values between all pairs of segments (i.e., $10 \times 10 = 100$). Finally, for the SN [18], we normalise computed cosine similarity scores. We adopt the VoxCeleb2 development set as the cohort set and then select the top 50,000 scores among cohort impostors to calculate the statistics for SN.

4.4. Implementation details

We implement models with the PyTorch library and conduct experiments using 4 NVIDIA GeForce RTX 3090 GPUs in

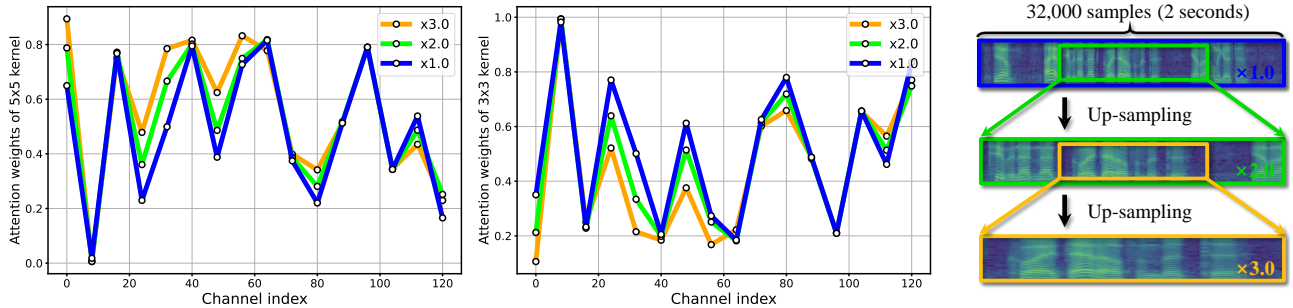


Figure 3: The attention weights of 5×5 (left) and 3×3 (middle) kernels for each 128 channel index. The 3 input utterances with different resolutions (right). The input utterance is randomly sampled from VoxCeleb1 test set (*id10272/dkN2DIBrXqQ/00002.wav*).

parallel¹. During training, we randomly crop an input utterance to a 2 seconds segment and then augment it with either MUSAN noises [19] or the simulated room impulse responses (RIRs) [20]. Input features to the models are 80-dimensional log mel-filterbanks derived with a hamming window length of 25ms and hop-size of 10ms with 512-size FFT bins. We apply mean and variance normalisation to the log mel-filterbanks [21].

The AAM-softmax objective function [17] adopts a margin of 0.2 and a scale of 30. For training, all models are trained with a batch size of 200 and optimised using an Adam optimiser [22] with a weight decay of $2e-5$. The learning rate was scheduled via the cosine annealing with warm-up restart [23] with a cycle size of 25 epochs, the maximum learning rate of $1e-3$ and the decreasing rate of 0.8 for two cycles.

5. Results

5.1. Main results

Table 1 describes the main experiments where we report several baselines and the proposed SKA-based models. We additionally report the evaluation result on short duration scenario. Speaker embedding extracted from a full duration of an enrolment utterance is compared with either a test utterance with 3 seconds or 1.5 seconds duration. We crop the middle part of an utterance to generate a short segment and if the utterance length is shorter than the target duration, we first duplicate and then perform cropping, following the protocol in [2, 24]. We also report the results using the three scoring approaches, i.e., the vanilla cosine similarity, TTA, SN, described in Section 4.3.

As depicted in rows 2 and 5 of Table 1, we observe marginal improvement by applying the proposed msSKA module in the backbone module (ECAPA-TDNN vs ECAPA-TDNN msSKA). Both models outperform the ResNet-based model (ResNet34 H/ASP), which are commonly used in the SV field. Next, we show that the use of the fcwSKA block-based front module (SKA-TDNN) boosts the performance compared to using the 2D-CNN or Res2Net-based front module (i.e., ECAPA-CNN-TDNN and MFA-TDNN). In addition, SKA-TDNN msSKA, including both fcwSKA block-based front module and msSKA block-based TDNN network, obtains further improved performance than the results of SKA-TDNN, achieving EER of 0.78% and MinDCF of 0.047 on the VoxCeleb-O test set, respectively.

We also investigate the effect of SKA-based models on test utterances with different duration. The proposed SKA-based

models show consistent relative improvement under all test scenarios on different duration. Compared to the SN results of best performing baseline, MFA-TDNN, on the VoxCeleb1-O test set, the SKA-TDNN obtains relative improvements of 5.17% and 13.64% in terms of EER on 3.0 seconds and 1.5 seconds test utterances, showing more improvement with shorter utterances.

Across all models including the proposed architectures, TTA and SN results show improved performance than those of typical cosine similarity where SN consistently showed the best performance on all evaluation sets.

5.2. Analysis and interpretation

We design an additional experiment to investigate further how the SKA module works. For this purpose, we observe the values of attention vectors (**a** and **b**) that decide on which kernel, either 3×3 or 5×5 , is more utilised when utterances with different resolutions are input. Utterances with different resolutions are generated using upsampling with interpolation as illustrated in the right side of Figure 3.

The left and the middle sides of Figure 3 illustrate attention weights of 5×5 kernel and 3×3 kernel using the utterance randomly sampled from the VoxCeleb1 test set. Comparing the original utterance (blue) with upsampled high resolution utterance (yellow), we observe that the attention weight for larger kernel becomes more activated. We hence confirm that the SKA module adaptively selects the kernel size, thereby selecting the receptive field size, adjusted in a *data-driven* fashion.

6. Conclusion

This paper introduces a selective kernel attention (SKA) module, allowing each convolutional layer to adaptively adjust kernel size based on an attention mechanism applied to both frequency and channel domain. In addition, we propose architectures by integrating the frequency-channel-wise SKA block-based front and the multi-scale SKA block-based TDNN networks, namely, ECAPA-TDNN msSKA, SKA-TDNN and SKA-TDNN msSKA. Vast experiments conducted using three different evaluation protocols demonstrate that both proposed SKA-based modules boost the verification performance and applying both modules simultaneously performed the best. The SKA modules are relatively robust to short duration scenarios.

7. Acknowledgements

We thank Bong-Jin Lee, Hee-Soo Heo, Young-ki Kwon, and You Jin Kim at Naver Corporation for valuable discussions.

¹All implementations are based on https://github.com/clovaai/voxceleb_trainer.

8. References

- [1] L. Wan, Q. Wang, A. Papir, and I. L. Moreno, "Generalized end-to-end loss for speaker verification," in *Proc. IEEE International Conference on Acoustics, Speech and Signal Processing (ICASSP)*. IEEE, 2018, pp. 4879–4883.
- [2] J.-w. Jung, H.-s. Heo, j.-h. Kim, H.-j. Shim, and H.-j. Yu, "RawNet: Advanced end-to-end deep neural network using raw waveforms for text-independent speaker verification," *Proc. Conference of the International Speech Communication Association (INTERSPEECH)*, pp. 1268–1272, 2019.
- [3] A. Nagrani, J. S. Chung, and A. Zisserman, "VoxCeleb: A large-scale speaker identification dataset," in *Proc. Conference of the International Speech Communication Association (INTERSPEECH)*, 2017, pp. 2616–2620.
- [4] J. S. Chung, A. Nagrani, and A. Zisserman, "VoxCeleb2: Deep speaker recognition," in *Proc. Conference of the International Speech Communication Association (INTERSPEECH)*, 2018, pp. 1086–1090.
- [5] J. S. Chung, J. Huh, S. Mun, M. Lee, H. S. Heo, S. Choe, C. Ham, S. Jung, B.-J. Lee, and I. Han, "In defence of metric learning for speaker recognition," in *Proc. Conference of the International Speech Communication Association (INTERSPEECH)*, 2020.
- [6] H. S. Heo, B.-J. Lee, J. Huh, and J. S. Chung, "Clova baseline system for the VoxCeleb Speaker Recognition Challenge 2020," *arXiv preprint arXiv:2009.14153*, 2020.
- [7] D. Snyder, D. Garcia-Romero, G. Sell, D. Povey, and S. Khudanpur, "X-vectors: Robust dnn embeddings for speaker recognition," in *Proc. IEEE International Conference on Acoustics, Speech and Signal Processing (ICASSP)*. IEEE, 2018, pp. 5329–5333.
- [8] J.-w. Jung, Y. J. Kim, H.-S. Heo, B.-J. Lee, Y. Kwon, and J. S. Chung, "Pushing the limits of raw waveform speaker recognition," *arXiv preprint:2203.08488*, 2022.
- [9] B. Desplanques, J. Thienpondt, and K. Demuynck, "ECAPA-TDNN: Emphasized Channel Attention, propagation and aggregation in TDNN based speaker verification," in *Proc. Conference of the International Speech Communication Association (INTERSPEECH)*, 2020, pp. 3830–3834.
- [10] J. Hu, L. Shen, and G. Sun, "Squeeze-and-excitation networks," in *Proc. IEEE/CVF Conference on Computer Vision and Pattern Recognition (CVPR)*, 2018, pp. 7132–7141.
- [11] S.-H. Gao, M.-M. Cheng, K. Zhao, X.-Y. Zhang, M.-H. Yang, and P. Torr, "Res2net: A new multi-scale backbone architecture," *IEEE Transactions on Pattern Analysis and Machine Intelligence*, vol. 43, no. 2, pp. 652–662, 2019.
- [12] J. Thienpondt, B. Desplanques, and K. Demuynck, "Integrating Frequency Translational Invariance in TDNNs and Frequency Positional Information in 2D ResNets to Enhance Speaker Verification," in *Proc. Conference of the International Speech Communication Association (INTERSPEECH)*, 2021, pp. 2302–2306.
- [13] T. Liu, R. K. Das, K. A. Lee, and H. Li, "MFA: TDNN with Multi-scale Frequency-channel Attention for Text-independent Speaker Verification with Short Utterances," *arXiv preprint arXiv:2202.01624*, 2022.
- [14] X. Li, W. Wang, X. Hu, and J. Yang, "Selective kernel networks," in *Proc. IEEE/CVF Conference on Computer Vision and Pattern Recognition (CVPR)*, 2019, pp. 510–519.
- [15] H. Zhang, C. Wu, Z. Zhang, Y. Zhu, H. Lin, Z. Zhang, Y. Sun, T. He, J. Mueller, R. Manmatha *et al.*, "ResNeSt: Split-attention networks," *arXiv preprint arXiv:2004.08955*, 2020.
- [16] R. Zhang, J. Wei, X. Lu, W. Lu, D. Jin, J. Xu, L. Zhang, Y. Ji, and J. Dang, "TMS: A Temporal Multi-scale Backbone Design for Speaker Embedding," *arXiv preprint arXiv:2203.09098*, 2022.
- [17] J. Deng, J. Guo, N. Xue, and S. Zafeiriou, "Arcface: Additive angular margin loss for deep face recognition," in *Proc. IEEE/CVF Conference on Computer Vision and Pattern Recognition (CVPR)*, 2019, pp. 4690–4699.
- [18] P. Matejka, O. Novotný, O. Plchot, L. Burget, M. D. Sánchez, and J. Cernocký, "Analysis of Score Normalization in Multilingual Speaker Recognition," in *Proc. Conference of the International Speech Communication Association (INTERSPEECH)*, 2017, pp. 1567–1571.
- [19] D. Snyder, G. Chen, and D. Povey, "MUSAN: A music, speech, and noise corpus," *arXiv preprint arXiv:1510.08484*, 2015.
- [20] T. Ko, V. Peddinti, D. Povey, M. L. Seltzer, and S. Khudanpur, "A Study on data augmentation of reverberant speech for robust speech recognition," in *Proc. IEEE International Conference on Acoustics, Speech and Signal Processing (ICASSP)*. IEEE, 2017, pp. 5220–5224.
- [21] D. Ulyanov, A. Vedaldi, and V. Lempitsky, "Instance normalization: The missing ingredient for fast stylization," in *Proc. IEEE/CVF Conference on Computer Vision and Pattern Recognition (CVPR)*, 2016, pp. 1–6.
- [22] D. P. Kingma and J. Ba, "Adam: A method for stochastic optimization," in *Proc. International Conference on Learning Representations (ICLR)*, 2015, pp. 1–15.
- [23] I. Loshchilov and F. Hutter, "SGDR: Stochastic gradient descent with warm restarts," in *Proc. International Conference on Learning Representations (ICLR)*, 2017, pp. 1–13.
- [24] J.-h. Kim, H.-j. Shim, J. Heo, and H.-j. Yu, "RawNeXt: Speaker verification system for variable-duration utterances with deep layer aggregation and extended dynamic scaling policies," *arXiv preprint:2112.07935*, 2022.